BEAM SPREADING AND EMITTANCE OSCILLATION OF AN INTENSE MAGNETIZED BEAM IN FREE SPACE*

Chun-xi Wang[†], Kwang-Je Kim, ANL, Argonne, IL 60439, USA
Jack G. Zhang, IIT, Chicago, IL 60616,USA

Abstract

Intense beams with large angular momentum have important applications in electron cooling and in producing flat beams suitable for ultrafast x-ray generation, Smith-Purcell radiators, and possibly for a future linear collider. To gain a basic understanding of the influence of beam angular momentum in an otherwise space-charge-dominated beam, the behavior of such a beam in free space will be examined here, in particular, beam spreading due to space-charge force, as well as emittance oscillation. Drift space is an important part of a split photoinjector and plays a significant role in emitance compensation of a high-brightness photoinjector.

INTRODUCTION

By immersing the cathode in a magnetic field, beam with (large) angular momentum can be created and is referred to as "magnetized" beam. High-intensity magnetized beams have important applications in electron cooling and flat-beam generation. The emittance oscillation of a non-magnetized beam in the drift space of a split photoinjector has some generic properties such as the "double minimum" feature [1], which has been explained by space-charge induced beam spreadings of individual slices [2]. Here, we generalize the technique used in [2] to examine the influence of beam angular momentum on beam spreading and emittance oscillation in drift space.

For a round beam in an axisymmetric channel, the beam envelope is governed by the reduced beam envelope equation [3, 4]

$$\hat{\sigma}'' + \frac{\kappa}{\beta^2\gamma^2}\,\hat{\sigma} - \frac{\kappa_s}{\beta^2\gamma^2}\frac{1}{\hat{\sigma}} - \frac{\epsilon^2}{\hat{\sigma}^3} = 0. \qquad (1)$$

where $\hat{\sigma} = \sqrt{\beta\gamma}\,\sigma$ is the reduced envelope, κ represents the external focusing, and perveance $\kappa_s = I/2I_A$ gives the space-charge defocusing. Here, we consider uniform non-accelerating channels with constant κ and κ_s. In a drift space, $\kappa = 0$ and κ_s decreases somewhat due to longitudinal debunching, which will be ignored here. The emittance ϵ is conserved and may contain two parts: thermal emittance and angular momentum. Although angular momentum is correlated motion and intrinsically different from random thermal emittance, from the beam envelope evolution point of view, these two types of emittances make no difference. In high-brightness photoinjectors, the thermal emittance is sufficiently small such that

a non-magnetized beam can be considered space-charge dominated. However, the existence of beam angular momentum qualitatively changed the property of the envelope equation by adding a significant emittance term. In the following, we present preliminary exploration of the effects of angular momentum. Because we will only consider non-accelerating beams, $\beta\gamma = 1$ is set in the following sections to simplify the notation. By the same token, we will use σ instead of $\hat{\sigma}$ for the reduced envelope as well.

BEAM SPREADING IN A UNIFORM NON-ACCELERATING CHANNEL

In a uniform non-accelerating channel, the coefficients in the beam envelope equation are all constants. The corresponding envelope Hamiltonian (with the setting $\beta\gamma = 1$)

$$H = \frac{p^2}{2} + \kappa\frac{\sigma^2}{2} - \kappa_s\ln(\sigma) + \frac{\varepsilon^2}{2\sigma^2} \qquad (2)$$

is a constant of motion, whose value can be expressed with the initial σ_0 and σ_0'. Thus, we have the first integral

$$\sigma'^2 + \kappa\sigma^2 - \kappa_s\ln\sigma^2 + \frac{\varepsilon^2}{\sigma^2} = \sigma_0'^2 + \kappa\sigma_0^2 - \kappa_s\ln\sigma_0^2 + \frac{\varepsilon^2}{\sigma_0^2}. \qquad (3)$$

The beam envelope is bounded by the potential well [4]. The lower bound is due to space-charge defocusing and emittance pressure. If any, the upper bound is due to external focusing. It reaches an extreme size σ_m at $\sigma' = 0$, which can be determined by

$$\sigma_0'^2 + \kappa\sigma_0^2 - \kappa_s\ln\sigma_0^2 + \frac{\varepsilon^2}{\sigma_0^2} = \kappa\sigma_m^2 - \kappa_s\ln\sigma_m^2 + \frac{\varepsilon^2}{\sigma_m^2}. \qquad (4)$$

Note that in drift space, i.e., without external focusing, $\sigma_m'' > 0$, there will be a beam waist for a converging beam. With external focusing, σ_m may be a minimum or maximum depending on the sign of σ_m''. From these equations, σ' can be solved as

$$\tilde{\sigma}' = \frac{\sigma'}{\sigma_m} = \pm\sqrt{\kappa\left(1 - \tilde{\sigma}^2\right) + \frac{\kappa_s}{\sigma_m^2}\ln\tilde{\sigma}^2 + \frac{\varepsilon^2}{\sigma_m^4}\left(1 - \frac{1}{\tilde{\sigma}^2}\right)}, \qquad (5)$$

where $\tilde{\sigma} \equiv \sigma/\sigma_m$. The sign depends on whether the beam is converging $(-)$ or diverging $(+)$. By integrating Eq. (5) we obtain the solution of the beam envelope as

$$s = \int_{\frac{\sigma_0}{\sigma_m}}^{1} \frac{\mathbf{sign}(\sigma_0')\,dx}{\sqrt{\kappa\left(1 - x^2\right) + \frac{\kappa_s}{\sigma_m^2}\ln\left(x^2\right) + \frac{\varepsilon^2}{\sigma_m^4}\left(1 - \frac{1}{x^2}\right)}}$$

$$+ \int_1^{\frac{\sigma}{\sigma_m}} \frac{\mathbf{sign}(\sigma')\,dx}{\sqrt{\kappa\left(1 - x^2\right) + \frac{\kappa_s}{\sigma_m^2}\ln\left(x^2\right) + \frac{\varepsilon^2}{\sigma_m^4}\left(1 - \frac{1}{x^2}\right)}}. \qquad (6)$$

This integral cannot be expressed with elementary functions. In the case $\kappa = \kappa_s = 0$, this integral yields the well-known hyperbola envelope for a bunch of free particles. For a space-charge dominated beam in free space ($\kappa = \epsilon = 0$), this integral yields the so-called universal beam-spreading curve for $\sigma/\sqrt{\kappa_s}$, which is independent of slice perveances. However, for a magnetized beam, there is a non-zero emittance term. Thus, the beam perveance can not be scaled away from the envelope equation. Therefore, beam spreading of a magnetized beam will have nontrivial dependence on beam perveance, and there is no universal beam-spreading curve anymore.

ENVELOPE EVOLUTIONS NEARBY A REFERENCE ENVELOPE

The relative motions of various beam slices are responsible for the variation of projected emittance in high-brightness photoinjectors. Thus, it is interesting to examine the evolution of envelopes nearby a reference envelope. Assuming small deviations, we expand a slice envelope around the reference envelope $(\bar{\sigma}, \bar{\sigma}')$ as

$$\begin{pmatrix} \sigma \\ \sigma' \end{pmatrix} = \begin{pmatrix} \bar{\sigma} \\ \bar{\sigma}' \end{pmatrix} + \sum_{\alpha} \begin{pmatrix} \partial_{q^\alpha} \bar{\sigma} \\ \partial_{q^\alpha} \bar{\sigma}' \end{pmatrix} \delta q^\alpha , \qquad (7)$$

where δq^α represents a small deviation in certain parameter q^α. Here, we consider the deviations in the initial values $\delta\sigma_0$ and $\delta\sigma_0'$, as well as the slice perveance $\delta\kappa_s$, assuming all slices have the same emittance and angular momentum.

To compute the partial derivatives with respect to σ_0, we take derivatives on both sides of Eq. (6) with respect to σ_0 and use Eq. (5) for simplification, which yields

$$0 = \frac{1}{\sigma'/\sigma_m} \partial_{\sigma_0} \frac{\sigma}{\sigma_m} - \frac{1}{\sigma_0'/\sigma_m} \partial_{\sigma_0} \frac{\sigma_0}{\sigma_m} + \frac{\partial_{\sigma_0}\sigma_m}{\sigma_m} F_x, \quad (8)$$

where F_x denotes the integral,

$$F_x = \int_{\frac{\sigma_0}{\sigma_m}}^{1} \frac{\mathbf{sign}(\sigma_0') \left[\frac{\kappa_s}{\sigma_m^2} \ln\left(x^2\right) + 2\frac{\varepsilon^2}{\sigma_m^4} \left(1 - \frac{1}{x^2}\right) \right] dx}{\left[k\left(1-x^2\right) + \frac{\kappa_s}{\sigma_m^2} \ln\left(x^2\right) + \frac{\varepsilon^2}{\sigma_m^4} \left(1 - \frac{1}{x^2}\right) \right]^{3/2}}$$
$$+ \int_{1}^{\frac{\sigma}{\sigma_m}} \frac{\mathbf{sign}(\sigma') \left[\frac{\kappa_s}{\sigma_m^2} \ln\left(x^2\right) + 2\frac{\varepsilon^2}{\sigma_m^4} \left(1 - \frac{1}{x^2}\right) \right] dx}{\left[k\left(1-x^2\right) + \frac{\kappa_s}{\sigma_m^2} \ln\left(x^2\right) + \frac{\varepsilon^2}{\sigma_m^4} \left(1 - \frac{1}{x^2}\right) \right]^{3/2}} .$$

Thus, $\partial_{\sigma_0}\sigma$ can be solved as

$$\partial_{\sigma_0}\sigma = \frac{\sigma'}{\sigma_0'} + \frac{\sigma'}{\sigma_m} \partial_{\sigma_0}\sigma_m \left(\frac{\sigma}{\sigma'} - \frac{\sigma_0}{\sigma_0'} - F_x \right), \qquad (9)$$

where $\partial_{\sigma_0}\sigma_m$ can be obtained by differentiating Eq. (4) as

$$\partial_{\sigma_0}\sigma_m = \frac{\kappa\sigma_0 - \kappa_s/\sigma_0 - \varepsilon^2/\sigma_0^3}{\kappa\sigma_m - \kappa_s/\sigma_m - \varepsilon^2/\sigma_m^3} = \frac{\sigma_0''}{\sigma_m''}, \qquad (10)$$

which is non-zero unless staying at equilibrium.

Similarly, taking derivatives on both sides of Eq. (6) with respect to σ_0' yields the derivative $\partial_{\sigma_0'}\sigma$. Combined with Eq. (9), they give the first two expressions in the following sets of four derivatives:

$$\partial_{\sigma_0}\sigma = \frac{1}{\sigma_0'} \left(\sigma' - \sigma_0'' \partial_{\sigma_0'}\sigma \right), \qquad (11)$$

$$\partial_{\sigma_0'}\sigma = \frac{\sigma_0\sigma' - \sigma_0'\sigma}{\sigma_m\sigma_m''} + \frac{\sigma_0'\sigma'}{\sigma_m\sigma_m''} F_x, \qquad (12)$$

$$\partial_{\sigma_0}\sigma' = \frac{1}{\sigma_0'} \left(\sigma'' - \sigma_0'' \partial_{\sigma_0'}\sigma' \right), \qquad (13)$$

$$\partial_{\sigma_0'}\sigma' = \frac{\sigma_0\sigma''}{\sigma_m\sigma_m''} - \frac{\sigma_0'(\sigma\sigma'' - \sigma_m\sigma_m'')}{\sigma_m''\sigma_m\sigma'} + \frac{\sigma_0'\sigma''}{\sigma_m\sigma_m''} F_x. \quad (14)$$

The last two expressions can be obtained by differentiating the first two expressions with respect to s. Clearly, these derivatives have the initial values $\partial_{\sigma_0}\sigma(0) = \partial_{\sigma_0'}\sigma'(0) = 1$ and $\partial_{\sigma_0'}\sigma(0) = \partial_{\sigma_0}\sigma'(0) = 0$. In the special case $\kappa = 0$ and $\varepsilon = 0$, these expressions reduce to the simple results of Eqs. (16) and (18) in [2], and $F_x = s$. It is important to note that, for a space-charge dominated beam where the emittance term can be neglected, all these expressions are independent of slice perveance, with or without external focusing. This property may play a significant role in emittance compensation of high-brightness photoinjectors. However, for a magnetized beam, these expressions will depend on the perveance of the (reference) slice.

To evaluate the effect of small perveance variations, we compute $\partial_{\kappa_s}\sigma$ and $\partial_{\kappa_s}\sigma'$ similarly. Differentiating Eqs. (3) and (4) yield, respectively,

$$\partial_{\kappa_s}\sigma' = \frac{1}{\sigma'} \left(\ln\frac{\sigma}{\sigma_0} + \sigma''\partial_{\kappa_s}\sigma \right), \qquad (15)$$

$$\partial_{\kappa_s}\sigma_m = \frac{1}{\sigma_m''} \ln\frac{\sigma_0}{\sigma_m}. \qquad (16)$$

Differentiating Eq. (6) with the help of function F_x and the above expression for $\partial_{\kappa_s}\sigma_m$ gives

$$\partial_{\kappa_s}\sigma = \frac{\sigma'}{\sigma_m\sigma_m''} \left(\frac{\sigma}{\sigma'} - \frac{\sigma_0}{\sigma_0'} - F_x \right) \ln\frac{\sigma_0}{\sigma_m} + \frac{\sigma'}{2} F_s, \quad (17)$$

where the function F_s is defined the same as F_x except that $\kappa_s = 1$ and $\epsilon = 0$ are set in the numerators. (Thus, for a space-charge dominated beam, $F_x = \kappa_s F_s$.) The initial values of both $\partial_{\kappa_s}\sigma$ and $\partial_{\kappa_s}\sigma'$ are zero.

EMITTANCE OSCILLATION

From the envelope expressions in Eq. (7), assuming the various deviations from the reference envelope are uncorrelated, the emittance due to slice envelope variations can be calculated as [2]

$$\epsilon^{\mathrm{env}} \simeq \sqrt{\sum_{\alpha} W_{q^\alpha}^2 \left(\overline{(\delta q^\alpha)^2} \Big/ \overline{q^\alpha}^2 \right)}, \qquad (18)$$

where

$$W_{q^\alpha} \equiv (\bar\sigma \partial_{q^\alpha} \bar\sigma' - \bar\sigma' \partial_{q^\alpha} \bar\sigma) \, \overline{q^\alpha}. \qquad (19)$$

Here, the bar over δq^α and q^α indicates averaging over the slices.

Inserting the above partial derivatives into Eq. (19), we have

$$W_\sigma = \bar\sigma_0 \left[\frac{\bar\sigma \bar\sigma'' - \bar\sigma'^2}{\bar\sigma_0'} \left(1 - \frac{\bar\sigma_0''}{\bar\sigma'} \partial_{\sigma_0'} \bar\sigma \right) - \frac{\bar\sigma \bar\sigma_0''}{\bar\sigma'} \right], \quad (20)$$

$$W_{\sigma'} = \bar\sigma_0' \left[\frac{\bar\sigma \bar\sigma'' - \bar\sigma'^2}{\bar\sigma'} \partial_{\sigma_0'} \bar\sigma + \frac{\bar\sigma \bar\sigma_0'}{\bar\sigma'} \right]. \qquad (21)$$

These expressions reduce to the special results of Eqs. (17) and (19) in [2]. Since $\partial_{\sigma_0'} \bar\sigma$ equals zero at the beginning, we have the initial values

$$W_\sigma(0) = -W_{\sigma'}(0) = -\bar\sigma_0 \bar\sigma_0'. \qquad (22)$$

To examine the extreme values of $W_\sigma(s)$ and $W_{\sigma'}(s)$, we take the s-derivative of these functions and have, after some algebra,

$$W_\sigma' = \bar\sigma_0 \frac{\bar\sigma \bar\sigma''' - \bar\sigma' \bar\sigma''}{\bar\sigma_0' \bar\sigma'} \left(\bar\sigma' - \bar\sigma_0'' \partial_{\sigma_0'} \bar\sigma \right), \qquad (23)$$

$$W_{\sigma'}' = \bar\sigma_0' \frac{\bar\sigma \bar\sigma''' - \bar\sigma' \bar\sigma''}{\bar\sigma'} \partial_{\sigma_0'} \bar\sigma. \qquad (24)$$

It is easy to see that the factor

$$\frac{\bar\sigma \bar\sigma''' - \bar\sigma' \bar\sigma''}{\sigma'} = -2 \left[\frac{\kappa_s}{\sigma} + 2 \frac{\varepsilon^2}{\sigma^3} \right] \neq 0,$$

thus W_σ reaches the extreme value of $-\bar\sigma_0 \bar\sigma_0'' \bar\sigma / \bar\sigma'$ when $\bar\sigma' = \bar\sigma_0'' \partial_{\sigma_0'} \bar\sigma$, and $W_{\sigma'}$ reaches the extreme value of $\bar\sigma_0'^2 \bar\sigma / \bar\sigma'$ when $\partial_{\sigma_0'} \bar\sigma = 0$. Using Eq. (12) and the condition for the extreme, we can further express the extreme values W_σ^{m} as

$$W_\sigma^{\mathrm{m}} = -\bar\sigma_0 \bar\sigma_0'' \frac{\bar\sigma}{\bar\sigma'} = \frac{\bar\sigma_0}{\bar\sigma_0'} (\bar\sigma_m \bar\sigma_m'' - \bar\sigma_0 \bar\sigma_0'') - \bar\sigma_0 \bar\sigma_0'' F_x, \quad (25)$$

$$W_{\sigma'}^{\mathrm{m}} = \bar\sigma_0'^2 \frac{\bar\sigma}{\bar\sigma'} = \bar\sigma_0 \bar\sigma_0' + \bar\sigma_0'^2 F_x \qquad (26)$$

where F_x integrates up to the extreme point. However, it is not obvious that the condition for the extremes can be satisfied (except the trivial case $W_{\sigma'}' = \partial_{\sigma_0'} \bar\sigma = 0$ at the beginning).

From these expressions, a few general properties can be drawn about emittance oscillation. In particular, for a beam focused into a drift, $\bar\sigma_0' < 0$, $\bar\sigma_0'' > 0$, $\bar\sigma_m \bar\sigma_m'' - \bar\sigma_0 \bar\sigma_0'' > 0$, thus $W_\sigma(0) > 0$ and $W_\sigma^m < 0$, which leads to emittance minimum when W_σ crosses zero, as discussed in [2]. Furthermore, $W_\sigma^m < 0$ requires $\bar\sigma' > 0$ at that location, thus the emittance maximum due to W_σ is always located after the beam waist where $\bar\sigma' = 0$.

Similarly, W_{κ_s} can be worked out as

$$W_{\kappa_s} = \bar\kappa_s \left[\frac{\bar\sigma}{\bar\sigma'} \ln \frac{\bar\sigma}{\bar\sigma_0} + \frac{\bar\sigma \bar\sigma'' - \bar\sigma'^2}{\bar\sigma'} \partial_{\kappa_s} \bar\sigma \right], \qquad (27)$$

where $\partial_{\kappa_s} \bar\sigma$ is given by Eq. (17). Clearly, $W_{\kappa_s}(0) = 0$.

EFFECTS OF BEAM ANGULAR MOMENTUM

To see the influence of beam angular momentum on the beam envelope spreading of an individual slice and on the emittance oscillation of a bunch of slices, we plot a set of five figures showing the quantities σ, σ', W_σ, $W_{\sigma'}$, and W_{κ_s}, using the expressions given above. In each figure, the red curve shows the evolution of a space-charge dominated beam and the blue curve shows the same beam but with an angular momentum term 10 times larger than the space-charge term at the beam waist (2 mm). The other parameters are $\sigma_0 = 9\,mm$, $\sigma' = -9.5\,mrad$, $\beta\gamma = 12$, $\kappa_s = 0.05$, which are adopted from an optimized SPARC photoinjector design.

Through this example and the above analysis, we see that, qualitatively speaking, the basic behavior of beam spreading and emittance oscillation in drift space are not changed by the large angular momentum, although there are significant quantitative changes. For example, the beam waist becomes much larger and is reached much quicker. Also, the emittance oscillation amplitude gets larger, and so on. From this point of view, W_{κ_s} may be an exception because there is no zero crossing anymore for the blue curve.

However, emittance compensation for magnetized beam [5] may be significantly different from conventional space-charge dominated beam. For example, there is no invariant envelope solution for the envelope equation in a booster when there is a significant emittance term. Thus, the matching condition for space-charge dominated beam may not be appropriate any more. Furthermore, the ability to compensate emittance may be limited by the fact that beam perveance cannot be scaled away from the envelope equation of a magnetized beam.

CONCLUDING REMARK

We developed a technique to examine the beam spreading and emittance oscillation of a magnetized beam in free space. Clearly, the technique also applies to a beam with significant thermal emittance and/or in a uniform focusing channel (we have kept both focusing κ and emittance ϵ in all the expressions). In a focusing channel, a beam may reach both minimum and maximum size because it is bounded by a potential well. For example, a diverging beam reaches a maximum beam size in the focusing solenoid for emittance compensation. The emittance evolution in the solenoid can be described by the same expressions presented above. Much more work is needed to understand emittance compensation of a magnetized beam.

REFERENCES

[1] M. Ferrario, J.E. Clendenin, D.T. Palmer, J.B. Rosenzweig, L. Serafini, SLAC-PUB-8400 (2000).

[2] C.-x. Wang, "Emittance oscillation in the drift space of split photoinjectors," Proceedings of the 35nd Advanced ICFA

Beam Dynamics Workshop on Physics and Application of High-Brightness Electron Beam, October 2005.

[3] See, for example, J.D. Lawson, *The Physics of Charged Particle Beams*, 2nd ed. (Oxford University Press, New York, 1988).

[4] C.-x. Wang, Nucl. Instrum. Methods A**557**, 94 (2006).
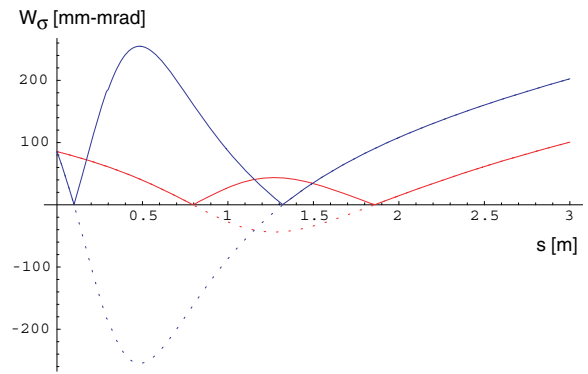
[5] X. Chang, I. Ben-Zvi, J. Kewisch, BNL-73192-2004-CP.

Figure 3: Emittance oscillation in free space due to initial slice envelope variation for space-charge dominated beam (red) and beam with large emittance (blue). The solid curves plot the absolute values.
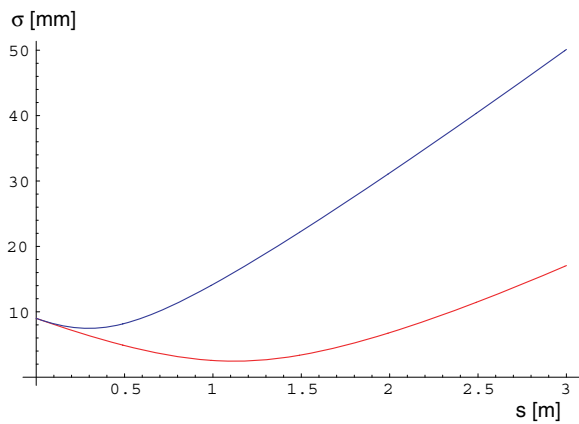
Figure 1: Reduced envelope in free space for space-charge dominated beam (red) and beam with large emittance (blue).
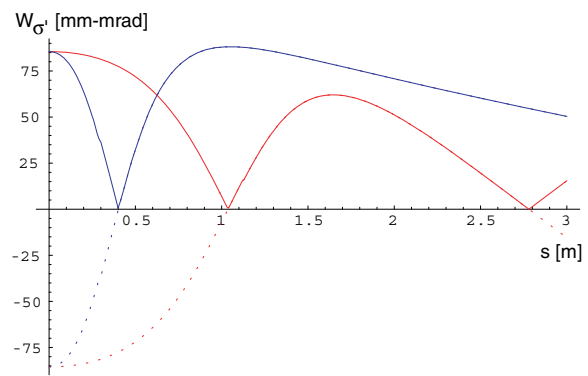

Figure 4: Emittance oscillation in free space due to initial slice slope variation for space-charge dominated beam (red) and beam with large emittance (blue). The solid curves plot the absolute values.
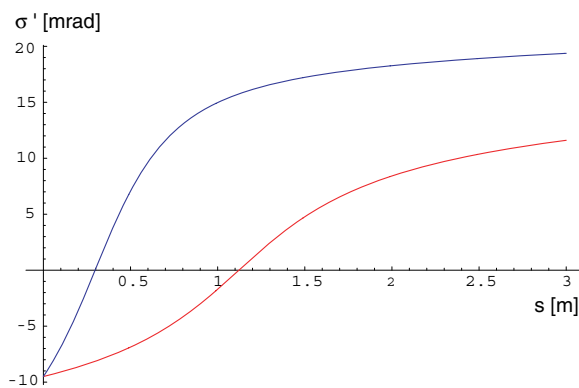

Figure 2: Reduced envelope slope in free space for space-charge dominated beam (red) and beam with large emittance (blue).
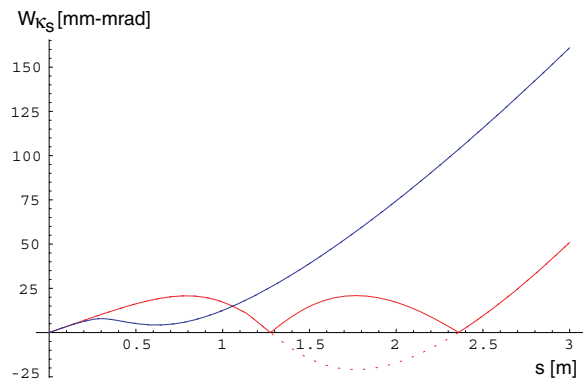

Figure 5: Emittance oscillation in free space due to slice perveance variation for space-charge dominated beam (red) and beam with large emittance (blue). The solid curves plot the absolute values.